An isotope dilution model for partitioning of phenylalanine and tyrosine uptake by the liver of lactating dairy cows

An isotope dilution model for partitioning of phenylalanine and tyrosine uptake by the liver of lactating dairy cows

L.A. Crompton[a,*], L.L. McKnight[b], C.K. Reynolds[a], J.A.N. Mills[a], J.L. Ellis[b,c], M.D. Hanigan[d], J. Dijkstra[c], B.J. Bequette[e,1] A. Bannink[c] and J. France[b]

[a] *Sustainable Agriculture and Food Systems Research Division, School of Agriculture, Policy and Development, University of Reading, Whiteknights, Reading RG6 6AR, UK*

[b] *Centre for Nutrition Modelling, Department of Animal Biosciences, University of Guelph, Ontario N1G 2W1, Canada*

[c] *Animal Nutrition Group, Wageningen University & Research, 6700 AH Wageningen, The Netherlands*

[d] *Department of Dairy Science, Virginia Tech, 2080 Litton Reaves, Blacksburg, VA 24061, USA*

[e] *Department of Animal & Avian Sciences, University of Maryland, College Park, MD 20742, USA*

[1]Deceased

[*]**Corresponding author:** l.a.crompton@reading.ac.uk (L.A. Crompton)

Abstract

An isotope dilution model to describe the partitioning of phenylalanine (PHE) and tyrosine (TYR) in the bovine liver was developed. The model comprises four intracellular and six extracellular pools and various flows connecting these pools and external blood. Conservation of mass principles were applied to generate the fundamental equations describing the behaviour of the system in the steady state. The model was applied to datasets from multi-catheterised dairy cattle during a constant infusion of [1-^{13}C] phenylalanine and [2,3,5,6-^{2}H] tyrosine tracers. Model solutions described the extraction of PHE and TYR from the liver via the portal vein and hepatic artery. In addition, the exchange of free PHE and TYR between extracellular and intracellular pools was explained and the hydroxylation of PHE to TYR was estimated. The model was effective in providing information about the fates of PHE and TYR in the liver and could be used as part of a more complex system describing amino acid metabolism in the whole animal.

Keywords:

Isotope dilution, Kinetic model, Liver, Phenylalanine, Tyrosine

1. Introduction

In ruminant production, the efficiency of milk protein synthesis from absorbed dietary nitrogen is quite low, 25-35 % (Hristov et al., 2004). In addition to the economic burden on the producer, urinary nitrogen losses contribute to greenhouse gas emissions and waterway contamination (Dijkstra et al., 2013). Milk protein synthesis is sensitive to essential amino acid supply, particularly phenylalanine (PHE). *In vivo* studies have demonstrated a reduction in milk protein concentrations when PHE is in low dietary supply (Rulquin and Pisulewski, 2000) and/or deficient in infusion mixtures (Doelman et al., 2015; Doepel et al., 2016). In the post-absorptive state, the liver has a key role in regulating PHE homeostasis. The liver can regulate the provision of PHE to peripheral tissues including the mammary gland, and remove PHE not used by the mammary gland or other peripheral tissues.

Net flux of PHE across the bovine liver has been examined *in vivo* using the arterio-venous difference technique (Tagari et al., 2004, 2008; Raggio et al., 2007; Berthiaume et al., 2006; Cantalapiedra-Hijar et al., 2014; Larsen et al., 2015). These studies reported a negative net flux of PHE, suggesting the liver is a major site of PHE utilization. In general, PHE has two metabolic fates, incorporation into protein or conversion to tyrosine (TYR) via PHE hydroxylase (oxidation). As a result, PHE catabolism always follows the pathway of TYR catabolism. Therefore, to examine PHE metabolism experimentally the simultaneous infusion of PHE and TYR stable isotope tracers is preferred. To resolve the kinetic data from such isotope infusion studies, mathematical models must be applied.

Mathematical models to describe PHE kinetics have varied in complexity (reviewed by Matthews, 2007). Simple models ignore the hydroxylation of PHE to TYR, whereas, more complex models aim to explain PHE conversion to TYR. In our previous publication (Crompton et al., 2014), we presented an eight pool compartmental model describing PHE and TYR metabolism in the mammary gland of lactating dairy cows. The present study is a

63 progression of this work and our previous model of leucine metabolism in the bovine liver
64 (France et al., 1998). The primary objective was to develop a steady state model of hepatic
65 PHE and TYR metabolism. The new model describes the partitioning of the PHE and TYR
66 between constitutive and export protein synthesis and potential other metabolic fates such as
67 hydroxylation of PHE to TYR.
68
69 **2. The model**
70 The scheme adopted is shown in Figure 1a. It contains four intracellular and six
71 extracellular pools. The intracellular pools are free PHE (pool 6), PHE in export protein
72 (pool 5), free TYR (pool 7) and TYR in export protein (pool 8), while the extracellular ones
73 represent portal vein PHE and TYR (pools 1 and 3), hepatic artery PHE and TYR (pools 2
74 and 4) and venous PHE and TYR (pools 9 and X). Pools external to the model and therefore
75 not specifically represented are indicated by the digit zero. The flows of PHE and TYR
76 between pools and into and out of the system are shown as arrowed lines.
77 The export protein-bound PHE pool has a single inflow: from free PHE, F_{56}, and two
78 efflows: secretion of export protein, F_{05}, and degradation, F_{65}. The intracellular free PHE
79 pool has four inflows: from the degradation of constitutive liver protein, F_{60}, from the
80 extracellular portal vein pool, F_{61}, from the hepatic artery pool, F_{62}, and from degradation of
81 export protein, F_{65}. The pool has four efflows: synthesis of constitutive liver protein, F_{06},
82 incorporation into export protein, F_{56}, hydroxylation to the intracellular free TYR pool, F_{76},
83 and outflow to the extracellular hepatic vein PHE pool, F_{96}. The intracellular free TYR pool
84 has five inflows: from the degradation of constitutive liver protein, F_{70}, from the extracellular
85 portal vein TYR pool, F_{73}, from the hepatic artery TYR pool, F_{74}, from the intracellular PHE
86 pool, F_{76}, and from the degradation of export protein, F_{78}. The pool has four efflows:
87 oxidation and TYR degradation products, $F_{07}^{(o)}$, synthesis of constitutive liver protein, $F_{07}^{(s)}$,

incorporation into export protein, F_{87}, and outflow to the extracellular hepatic vein TYR pool, F_{X7}. The export protein-bound TYR pool has one inflow: from the intracellular free TYR pool, F_{87}, and two efflows: secretion of export protein, F_{08}, and degradation, F_{78}.

The extracellular portal vein PHE pool has a single inflow: entry into the pool, F_{10}, and two efflows: uptake by the liver, F_{61}, and bypass to the extracellular hepatic vein PHE pool, F_{91}. The extracellular hepatic artery PHE pool has a single inflow: entry into the pool, F_{20}, and two efflows: uptake by the liver, F_{62}, and bypass to the extracellular hepatic vein PHE pool, F_{92}. The same description applies to the corresponding TYR pools, i.e. pools 3 and 4 with flows F_{30}, F_{73}, F_{X3}, F_{40}, F_{74}, and F_{X4}, respectively. The extracellular hepatic vein PHE pool has three inflows: bypass from the portal vein PHE pool, F_{91}, bypass from the hepatic artery PHE pool, F_{92}, and release from the intracellular PHE pool, F_{96}, and one efflow from the system, F_{09}. The same description applies to the corresponding TYR pool with flows F_{X3}, F_{X4}, F_{X7}, and F_{0X} respectively.

The schemes adopted for the movement of label are shown in Figures 1b and 1c. Labelled [1-^{13}C]PHE and [2,3,5,6-^{2}H]TYR were infused into the jugular vein at a constant rate for 8 h.. The enrichments of the extracellular pools are measured directly by taking blood samples from the portal vein, hepatic artery and hepatic vein during the isotope infusion. The enrichments of the intracellular pools can only be measured directly using invasive procedures and to avoid such procedures, the enrichments of the intracellular pools were set as a prescribed fraction of the corresponding arterial enrichment in this study. Blood flow rate across the liver is measured by downstream dye dilution using *para*-amino hippuric acid (PAH), but uncorrected for any N-acetylation that occurs across the liver (Katz and Bergman, 1969). The scheme assumes that the only entry of label into the system is into the PHE and TYR portal vein and hepatic artery pools via the effective infusion rates, flows I_1,

I_2, I_3, Φ_3, I_4, and Φ_4 and that the duration of the infusion is such that no label arises from the breakdown of constitutive protein.

Conservation of mass principles can be applied to each pool in Figure 1a, b, c to generate differential equations that describe the dynamic behaviour of the system. For total (isotopic plus non-isotopic) PHE and TYR, these fundamental equations are (mathematical notation is defined in Table 1):

$$\frac{\mathrm{d}Q_1}{\mathrm{d}t} = F_{10} - F_{61} - F_{91} \tag{1}$$

$$\frac{\mathrm{d}Q_2}{\mathrm{d}t} = F_{20} - F_{62} - F_{92} \tag{2}$$

$$\frac{\mathrm{d}Q_3}{\mathrm{d}t} = F_{30} - F_{73} - F_{\mathrm{X}3} \tag{3}$$

$$\frac{\mathrm{d}Q_4}{\mathrm{d}t} = F_{40} - F_{74} - F_{\mathrm{X}4} \tag{4}$$

$$\frac{\mathrm{d}Q_5}{\mathrm{d}t} = F_{56} - F_{05} - F_{65} \tag{5}$$

$$\frac{\mathrm{d}Q_6}{\mathrm{d}t} = F_{60} + F_{61} + F_{62} + F_{65} - F_{06} - F_{56} - F_{76} - F_{96} \tag{6}$$

$$\frac{\mathrm{d}Q_7}{\mathrm{d}t} = F_{70} + F_{73} + F_{74} + F_{76} + F_{78} - F_{07}^{(o)} - F_{07}^{(s)} - F_{87} - F_{\mathrm{X}7} \tag{7}$$

$$\frac{\mathrm{d}Q_8}{\mathrm{d}t} = F_{87} - F_{08} - F_{78} \tag{8}$$

$$\frac{\mathrm{d}Q_9}{\mathrm{d}t} = F_{91} + F_{92} + F_{96} - F_{09} \tag{9}$$

$$\frac{\mathrm{d}Q_{\mathrm{X}}}{\mathrm{d}t} = F_{\mathrm{X}3} + F_{\mathrm{X}4} + F_{\mathrm{X}7} - F_{0\mathrm{X}} \tag{10}$$

and for [^{13}C] labelled PHE and TYR:

$$\frac{\mathrm{d}q_1}{\mathrm{d}t} = I_1 - e_1\left(F_{61} + F_{91}\right) \tag{11}$$

$$\frac{\mathrm{d}q_2}{\mathrm{d}t} = I_2 - e_2\left(F_{62} + F_{92}\right) \tag{12}$$

$$\frac{\mathrm{d}q_3}{\mathrm{d}t} = I_3 - e_3\left(F_{73} + F_{\mathrm{X}3}\right) \tag{13}$$

$$\frac{\mathrm{d}q_4}{\mathrm{d}t} = I_4 - e_4\left(F_{74} + F_{\mathrm{X}4}\right) \tag{14}$$

$$\frac{\mathrm{d}q_5}{\mathrm{d}t} = e_6F_{56} - e_5\left(F_{05} + F_{65}\right) \tag{15}$$

$$\frac{\mathrm{d}q_6}{\mathrm{d}t} = e_1F_{61} + e_2F_{62} + e_5F_{65} - e_6\left(F_{06} + F_{56} + F_{76} + F_{96}\right) \tag{16}$$

$$\frac{\mathrm{d}q_7}{\mathrm{d}t} = e_3F_{73} + e_4F_{74} + e_6F_{76} + e_8F_{78} - e_7\left(F_{07}^{(o)} + F_{07}^{(s)} + F_{87} + F_{\mathrm{X}7}\right) \tag{17}$$

$$\frac{\mathrm{d}q_8}{\mathrm{d}t} = e_7F_{87} - e_8\left(F_{08} + F_{78}\right) \tag{18}$$

$$\frac{\mathrm{d}q_9}{\mathrm{d}t} = e_1F_{91} + e_2F_{92} + e_6F_{96} - e_9F_{09}$$

(19)

$$\frac{\mathrm{d}q_{\mathrm{X}}}{\mathrm{d}t} = e_3F_{\mathrm{X}3} + e_4F_{\mathrm{X}4} + e_7F_{\mathrm{X}7} - e_{\mathrm{X}}F_{0\mathrm{X}} \tag{20}$$

and for [^{2}H] labelled TYR:

$$\frac{\mathrm{d}\phi_3}{\mathrm{d}t} = \Phi_3 - \varepsilon_3\left(F_{73} + F_{\mathrm{X}3}\right)$$

(21)

$$\frac{\mathrm{d}\phi_4}{\mathrm{d}t} = \Phi_4 - \varepsilon_4\left(F_{74} + F_{\mathrm{X}4}\right) \tag{22}$$

$$\frac{\mathrm{d}\phi_7}{\mathrm{d}t} = \varepsilon_3F_{73} + \varepsilon_4F_{74} + \varepsilon_8F_{78} - \varepsilon_7\left(F_{07}^{(o)} + F_{07}^{(s)} + F_{87} + F_{\mathrm{X}7}\right) \tag{23}$$

$$\frac{\mathrm{d}\phi_8}{\mathrm{d}t} = \varepsilon_7F_{87} - \varepsilon_8\left(F_{08} + F_{78}\right) \tag{24}$$

$$\frac{\mathrm{d}\phi_{\mathrm{X}}}{\mathrm{d}t} = \varepsilon_3F_{\mathrm{X}3} + \varepsilon_4F_{\mathrm{X}4} + \varepsilon_7F_{\mathrm{X}7} - \varepsilon_{\mathrm{X}}F_{0\mathrm{X}} \tag{25}$$

When the system is in steady state with respect to both total and labelled PHE and TYR, the derivative terms in equations (1)-(25) are zero. For the scheme assumed, the enrichment of intracellular export protein-bound pools equalizes with that of the respective free pool in steady state (i.e. $e_5 = e_6$, $e_8 = e_7$, $\varepsilon_8 = \varepsilon_7$) otherwise equations (5) and (15), and (8), (18) and (24) are inconsistent. It should be noted that the liver is a heterogeneous mixture of cells, and enrichment may differ at different parts of the organ where synthesis of export protein or synthesis of constitutive protein takes place. Within cells there are different sites of synthesis and oxidation, and differences in the sites of synthesis of individual proteins, with labelling of the tracer amino acid highest at points near the cell surface and lowest at points near the sites of degradation (see Waterlow, 2006). After equating intracellular enrichments and eliminating redundant equations etc., equations (11) to (25) yield the following useful identities:

$$I_1 - e_1\left(F_{61} + F_{91}\right) = 0 \tag{26}$$

$$I_2 - e_2\left(F_{62} + F_{92}\right) = 0 \tag{27}$$

$$e_1F_{61} + e_2F_{62} - e_6\left(F_{06} + F_{56} + F_{76} + F_{96} - F_{65}\right) = 0 \tag{28}$$

$$e_3F_{73} + e_4F_{74} + e_6F_{76} - e_7\left(F_{07}^{(o)} + F_{07}^{(s)} + F_{87} + F_{X7} - F_{78}\right) = 0 \tag{29}$$

$$e_1F_{91} + e_2F_{92} + e_6F_{96} - e_9F_{09} = 0 \tag{30}$$

$$e_3F_{X3} + e_4F_{X4} + e_7F_{X7} - e_XF_{0X} = 0 \tag{31}$$

$$\Phi_3 - \varepsilon_3\left(F_{73} + F_{X3}\right) = 0 \tag{32}$$

$$\Phi_4 - \varepsilon_4\left(F_{74} + F_{X4}\right) = 0 \tag{33}$$

$$\varepsilon_3F_{73} + \varepsilon_4F_{74} - \varepsilon_7\left(F_{07}^{(o)} + F_{07}^{(s)} + F_{87} + F_{X7} - F_{78}\right) = 0 \tag{34}$$

$$\varepsilon_3F_{X3} + \varepsilon_4F_{X4} + \varepsilon_7F_{X7} - \varepsilon_XF_{0X} = 0 \tag{35}$$

To obtain steady state solutions to the model, it is assumed that PHE and TYR secreted in export protein, CO_2 production and PHE and TYR removal from the hepatic vein pools (i.e. F_{05}, F_{08}, $F_{07}^{(o)}$, F_{09} and F_{0X}, respectively) can all be measured experimentally. Further, it is mathematically convenient to assume that percentage PHE extraction by the liver is the same from the portal vein and hepatic artery supplies, giving:

$$\frac{F_{91}}{F_{92}}\left(=\frac{F_{61}}{F_{62}}\right)=\frac{F_{10}}{F_{20}} \tag{36}$$

Algebraic manipulation of equations (1)-(10) with the derivatives set to zero, together with equations (26)-(36), gives the following unique solution:

$$F_{10}=I_1/e_1 \tag{37}$$

$$F_{20}=I_2/e_2 \tag{38}$$

$$F_{30}=\Phi_3/\varepsilon_3 \tag{39}$$

$$F_{40}=\Phi_4/\varepsilon_4 \tag{40}$$

$$\overline{F_{56}-F_{65}}=\widetilde{F}_{05} \tag{41}$$

$$\overline{F_{87}-F_{78}}=\widetilde{F}_{08} \tag{42}$$

$$F_{X7}=\frac{(e_4-e_3)(\varepsilon_X-\varepsilon_3)-(e_X-e_3)(\varepsilon_4-\varepsilon_3)}{(e_4-e_3)(\varepsilon_7-\varepsilon_3)-(e_7-e_3)(\varepsilon_4-\varepsilon_3)}\widetilde{F}_{0X} \tag{43}$$

$$F_{X4}=\frac{(\varepsilon_X-\varepsilon_3)\widetilde{F}_{0X}-(\varepsilon_7-\varepsilon_3)F_{X7}}{(\varepsilon_4-\varepsilon_3)} \tag{44}$$

$$F_{X3}=\widetilde{F}_{0X}-F_{X4}-F_{X7} \tag{45}$$

$$F_{73}=F_{30}-F_{X3} \tag{46}$$

$$F_{74}=F_{40}-F_{X4} \tag{47}$$

$$F_{07}^{(s)}=\frac{\varepsilon_3}{\varepsilon_7}F_{73}+\frac{\varepsilon_4}{\varepsilon_7}F_{74}-\widetilde{F}_{07}^{(o)}-\overline{F_{87}-F_{78}}-F_{X7} \tag{48}$$

189 $$F_{76} = \frac{e_7}{e_6}\left(\widetilde{F}_{07}^{(o)} + F_{07}^{(s)} + \overline{F_{87} - F_{78}} + F_{X7}\right) - \frac{e_3}{e_6}F_{73} - \frac{e_4}{e_6}F_{74} \quad (49)$$

190 $$F_{70} = \widetilde{F}_{07}^{(o)} + F_{07}^{(s)} + \overline{F_{87} - F_{78}} + F_{X7} - F_{73} - F_{74} - F_{76} \quad (50)$$

191 $$F_{91} = \frac{\left(e_9 - e_6\right)\widetilde{F}_{09}}{\left(e_1 - e_6\right) + \left(e_2 - e_6\right)\frac{F_{20}}{F_{10}}} \quad (51)$$

192 $$F_{92} = \frac{F_{20}}{F_{10}}F_{91} \quad (52)$$

193 $$F_{96} = \widetilde{F}_{09} - F_{91} - F_{92} \quad (53)$$

194 $$F_{61} = F_{10} - F_{91} \quad (54)$$

195 $$F_{62} = F_{20} - F_{92} \quad (55)$$

196 $$F_{06} = \frac{e_1}{e_6}F_{61} + \frac{e_2}{e_6}F_{62} - \overline{F_{56} - F_{65}} - F_{76} - F_{96} \quad (56)$$

197 $$F_{60} = F_{06} + \overline{F_{56} - F_{65}} + F_{76} + F_{96} - F_{61} - F_{62} \quad (57)$$

198 where for these equations the italics denote steady state values of flows and enrichments, the
199 tilde identifies a measured flow, and the over-lining (not to be confused with statistical mean)
200 indicates coupled flows (which cannot be separately estimated within the model). Equations
201 (37)-(57) were obtained through analytical solution (solving by hand) using conventional
202 linear algebra.
203

204 **3. Application**

205 Application of the model is illustrated using data from an experiment conducted in the
206 UK at the University of Reading with multi-catheterised mid-lactation Holstein-Friesian dairy
207 cows (average live-weight 667 kg). Animals were fed hourly by auto-feeders total mixed
208 ration (TMR) diets consisting of a 50:50 mixture on a dry matter basis of forage and
209 concentrate with the forage comprised of grass silage and chopped dried Lucerne in a 25:75

ratio on a dry matter basis. Concentrates were formulated to provide crude protein levels of approximately 110 and 200 g per kg concentrate dry matter, such that average TMR crude protein concentrations were 128 and 175 g/kg dry matter. Average daily dry matter intake and milk yield for these animals were 22 kg/d and 30 L/d, respectively. The cows were given constant abomasal infusions of water (18 L/d) for 4 d, followed by a buffered mixture of essential amino acids for a further 6 d. The essential amino acids were administered at a daily rate equivalent to the essential amino acids in 800 g milk protein. On the final day of each abomasal infusion, animals received a primed, continuous infusion at a constant rate into the jugular vein of [1-^{13}C]PHE (350 mg/h) and [2,3,5,6-^{2}H]TYR (100 mg/h) in sterile saline for 8 h. Blood samples were taken simultaneously from catheters in the dorsal aorta and the portal and hepatic veins at hourly intervals for the duration of the infusion for the measurement of blood flow rate (by PAH dilution) and nutrient metabolism by the portal drained viscera and liver. The final four blood samples taken 5-8 h after the infusion started were averaged to provide steady state values.

The relevant experimental measurements are given in Table 2. They are reported for three animals during the water infusion (2 low protein; 1 high protein diet) and one animal during the amino acid infusion (high protein diet). Values are based on plasma rather than whole blood. Phenylalanine and TYR measurements are based on free rather than total (i.e. free plus bound) plasma PHE and TYR. The effective isotope infusion rates to the liver, I_1, I_2, and I_3, Φ_3, I_4, Φ_4 were obtained from portal vein and arterial concentration and enrichment of PHE and TYR and plasma flow rate in the portal vein and hepatic artery. The flows F_{09} and F_{0X} were determined from hepatic vein PHE and TYR concentration and plasma flow rate in the hepatic vein. The intracellular enrichments e_6, e_7 and ε_7 and the flows F_{05}, F_{08} were not measured in the trial and had to be prescribed. Unpublished observations from our laboratories demonstrated an intracellular to extracellular enrichment ratio of 0.3 for PHE and

TYR. Therefore, the missing intracellular free PHE and TYR enrichments, $e_{6,}$ e_7, and ε_7 were initially calculated as 0.3 times the corresponding arterial enrichments $e_{2,}$ e_4, and ε_4 respectively. The export protein flows F_{05} and F_{08} were assigned values of 33.8 μmol/min and 25.0 μmol/min respectively based on Raggio et al. (2007) and the relative proportion of PHE and TYR in bovine serum albumin as a representative export protein (UniProt, 2017). The flow $F_{07}^{(o)}$ was obtained from labelled CO_2 elevation in plasma flow across the liver and hepatic vein PHE enrichment in sheep (Harris et al., 1992).

Calculated flows are presented in Table 3. Data provided were insufficient for comprehensive statistical analysis; therefore the results must be interpreted with a degree of caution. Initial solutions for each cow were non-physiological as some of the derived flows gave negative values. Therefore, error bands of ±25% were placed around the values given in Table 2 of the prescribed intracellular enrichments (e_6, e_7 and ε_7) and the measured extracellular enrichments close to minimum detection levels (e_3, e_4 and e_X), and the solution space mapped out by these bands was searched to find the best feasible solution for each cow. The best feasible solution was obtained by sum of squares minimisation, where the sum of squares to be minimised (SS) was defined as

$$\mathrm{SS} = \left(1 - \frac{F_{60}}{F_{06}}\right)^2 + \left(1 - \frac{F_{70}}{F_{07}^{(s)}}\right)^2 + \left(\frac{F_{07}^{(s)}}{F_{06}} - \frac{F_{70}}{F_{60}}\right)^2$$

The assumptions underlying SS are constitutive liver protein synthesis and degradation are moving towards equilibrium (as the cows were in mid-lactation), and the TYR to PHE ratio is the same (or similar) in synthesised and degraded liver tissue. If no feasible solution could be found, the error bands were expanded (up to ±40%) and the search repeated. The final solutions are shown in Table 3.

An analysis of measurement errors in experimental enrichments and infusion rates on model solutions was conducted. Mean values across all datasets were assigned to e_1, e_2, e_3,

e_4, e_6, e_7, e_9, e_x, ε_3, ε_4, ε_7, ε_x, I_1, I_2, Φ_3, Φ_4, F_{05}, $F_{07}^{(o)}$, F_{08}, F_{09}, F_{0X}. Inputs were then perturbed in turn by 0, ±10% and ±20%. Each calculated flow (y, μmol/min) was then plotted against the perturbation (x, %), and a five-point linear regression of y on x performed to determine the slope of the line produced. The average slope was subsequently scaled by its corresponding unperturbed average flow value, giving the scaled slopes dimensions of % change in y per % change in x. Results of the error assessment are presented in Table 4. In general, errors in infusion rates and measured flows had little impact on the sensitivity of model solutions. However, errors in the measurement of isotopic enrichment and in assumed intracellular enrichment values, cause marked changes in calculated flows, emphasising the value of measuring intracellular enrichment directly.

5. Discussion

Improving nitrogen utilization in the ruminant, and consequently minimizing the environmental impacts of ruminant production, is dependent on a clear understanding of post-absorptive amino acid metabolism. The present model described the partitioning of the indispensable amino acid, PHE (and TYR), in the bovine liver. The model gave estimates of PHE flow across the liver, rates of PHE and TYR incorporation into constitutive and export protein synthesis, and the rate of hydroxylation of PHE to TYR.

PHE and TYR enter the liver via the portal vein and hepatic artery. Amino acids entering via the portal vein, the main blood supply to liver, represent recently absorbed or released amino acids from the portal drained viscera and recirculating amino acids coming from the mesenteric and hepatic arteries. Incoming amino acids via arterial blood reflect the utilization of nutrients by peripheral tissues (Reynolds, 2006). The model predicted a greater flow of PHE and TYR from the portal vein (90% of total inflow) than that from the hepatic

283 artery, which was expected as the portal vein accounted for the majority (84%) of liver blood
284 flow.

285 *In vivo* studies have observed a negative net flow of PHE across the bovine liver,
286 suggesting the liver is a major site of catabolism (Tagari et al., 2004, 2008; Reynolds, 2006;
287 Raggio et al., 2007; Berthiaume et al., 2006; Cantalapiedra-Hijar et al., 2014; Larsen et al.,
288 2015). In agreement, model solutions indicated a net negative flow of PHE and TYR across
289 the liver (efflow minus inflow, –396 and –298 μmol/min PHE and TYR respectively). Other
290 efflows of PHE and TYR from the liver included oxidation and incorporation into secreted
291 hepatic proteins. Oxidation rates varied greatly in individual animals (range 146 to 525
292 μmol/min), the highest value observed in the animal receiving the essential amino acid
293 infusion. The range of oxidation rates in animals receiving the control water infusion were
294 similar to those previously reported in lactating dairy cows (Raggio et al., 2007) fed low and
295 high protein diets. Oxidation rates used in the present model represent the sum of PHE and
296 TYR oxidation and combined PHE and TYR oxidation accounted for 23% of total PHE and
297 TYR inflow to the liver. However, the current model enables the conversion of PHE to TYR
298 to be estimated (F_{76}) which enables the combined oxidation to be separated. Phenylalanine
299 may either be used for protein synthesis or be converted to TYR which is catalysed by the
300 enzyme phenylalanine hydroxylase and is the first and rate limiting step in the metabolic
301 disposal of PHE. Tyrosine is then transaminated to *p*-hydroxyphenylpyruvate and ultimately
302 yields fumarate and acetoacetate, so that PHE and TYR give rise to both glucogenic and
303 ketogenic fragments. Tyrosine is not considered essential, because it can be synthesised from
304 PHE in addition to that provided from the diet. On average the model estimated that 23% of
305 inflow of PHE from blood (sum of hepatic artery and portal vein inflows) to the liver was
306 converted to TYR. Of the 178 μmol/min of PHE hydroxylated, 101 μmol/min were directly
307 oxidised and 77 μmol/min contributed 11% of the 717 μmol/min total TYR inflow (sum of

TYR from hepatic artery and portal vein and from PHE hydroxylation). Individual amino acid oxidations as a percentage of liver inflow were estimated to be 13% for PHE and 29% for TYR. Measuring TYR oxidation directly represents a challenge experimentally. In general, deuterium labelled PHE is inadequate for quantifying PHE kinetics and oxidation, which requires the use of carbon labelled PHE and by default, deuterium labelled TYR (reviewed by Matthews, 2007).

Another efflow of PHE and TYR considered in the model was their incorporation into hepatic export protein. The liver makes several export proteins of various functions. Albumin is important for the maintenance of vascular osmotic pressure. Due to this critical role, albumin synthesis is maintained across various mild physiological challenges, although in more severe situations of nutrient shortage, albumin synthesis may decrease. Raggio et al. (2007) determined export plasma protein synthesis rate in lactating dairy cows and assumed that export plasma protein contained 5% PHE. The value thus obtained by Raggio et al. (2007) was used in the present model to represent the flow of PHE into export protein (F_{05}). Since plasma proteins are also derived from sources other than the liver, the assumption that total plasma export protein synthesis is all hepatic in origin may well have overestimated the flow of PHE into export protein to some degree in the current model. The incorporation of TYR (F_{08}) into albumin was unknown and assumed equivalent to that of PHE after correcting for the relative proportions of PHE and TYR in albumin. This assumption is recognized as a limitation of the current modelling exercise. Specifically, the incorporation of individual amino acids depends on the type of export protein; some export proteins may require proportionally higher amounts of PHE or TYR. This limitation was circumvented in our bovine mammary model (Crompton et al., 2014) as the export protein was milk and isotope enrichment in milk was easily measured.

A unique feature of the present model is the description of intracellular PHE and TYR partitioning. Constitutive hepatic protein degradation was the largest contributor to the free PHE and TYR pools, followed by portal vein and hepatic artery delivery (PHE 72%, 22%, 6%; TYR 65%, 22%, 5%). It should be noted that these estimates are influenced by assumptions which had to be made with respect to intracellular enrichments, as discussed later. Flow of PHE and TYR into constitutive protein synthesis comprised 98% of total synthetic flow. The ratio of PHE to TYR in synthesised constitutive protein and degraded constitutive protein was the same in each animal (range 1.06 to 1.66) and averaged 1.30. The ratio of constitutive protein synthesis to degradation was 1.1 for both PHE and TYR. However, in mid to late lactation dairy cows, the ratio of PHE and TYR synthesis to degradation should be equal. Model estimates of intracellular PHE and TYR partitioning must be interpreted with caution due to methodological limitations and imposed assumptions. For example, samples were taken from whole blood and free PHE and TYR concentrations were quantified and considered in the model. Therefore the extent to which peptide bound PHE and TYR contribute to constitutive protein synthesis and degradation flows cannot be determined. As hepatic tissues were not sampled, isotopic enrichment of the intracellular pools was estimated based on the sampled precursor pools. The choice of precursor pool enrichment is central in the present model as with any measurement of protein synthetic rate in the whole body or tissues (see Waterlow, 2006). The assumption that intracellular enrichments were 0.30 of plasma was based on unpublished observations from an unrelated in vivo trial from our laboratory. Using the same isotopes as the present study, average liver homogenate free enrichment for PHE and TYR was 0.30 (SD 0.07; range 0.19-0.38) of plasma enrichment in lactating dairy cattle. Initially, the model solved to give some non-physiological flows and had to be re-solved by adjusting the intracellular enrichments and the extracellular ones close to minimum detection levels using a least-squares minimisation

routine. Besides, the actual precursor pool for various constitutive and export proteins may differ. The lack of homogeneity in activity at various parts of the liver indicates that intracellular enrichment is not uniform throughout the liver, and enrichment in export protein and constitutive protein therefore may differ. In particular, the precursor enrichment for constitutive protein synthesis may be lower than that for export protein synthesis (Connell et al., 1997). Due to lack of specific measurements, this observation could not be included in the present model.

Another means of estimating intracellular enrichment would be to measure the incorporation of label into proteins having a fast turnover rate in plasma. For example, studies in humans use plasma VLDL apolipoprotein-B (Apo-B) enrichment as a hepatic intracellular marker protein (Rafi et al., 2008). However, to our knowledge this approach has not been undertaken in lactating dairy cattle and would likely yield the enrichment of the precursor pool used for export protein synthesis, which is not necessarily the same as the precursor pool for constitutive protein synthesis as discussed above.

5. Conclusions

The present 10-pool model allows for quantitative interpretation of the metabolism of PHE and TYR in the liver of dairy cattle by showing their partition among different fates. The model builds upon the existing eight pool model to describe protein turnover in the mammary gland of the lactating dairy cow (Crompton et al., 2014). The exchange of PHE and TYR between extracellular and intracellular pools was described and the hydroxylation of PHE to TYR was estimated. In addition, the extraction of amino acids from the liver via the portal vein and hepatic artery pools was represented. Upon application to dairy cattle during infusion of [1-^{13}C] phenylalanine and [2,3,5,6-^{2}H] tyrosine tracers, the model was shown to be effective in providing information about the fates of PHE and TYR in the liver, and could

be used as part of a more complex system describing amino acid metabolism in the whole animal.

Just as accurate measurements of precursor pool enrichment are critical for the use of labelled amino acids to determine tissue protein synthesis generally, the measurement of intracellular free PHE and TYR enrichment are crucial components of the present model, yet had to be estimated along with liver export protein in order to apply the model using the data available from the experiment. If the model is to be applied more rigorously, future *in vivo* studies should measure simultaneously the intracellular free PHE and TYR pools and liver export protein, along with the plasma enrichments and flow rates measured in the present work. Furthermore, the model could not be solved by algebraic means alone, as initially it solved to give non-physiological flows and had to be re-solved by adjusting selected enrichments using a least-squares minimisation routine. Therefore, the mathematical exercise of cleaving the combined model and solving the PHE and TYR sub-models independently but sequentially merits future investigation.

Acknowledgements

This work was funded, in part, through DEFRA project LS3656, the European Union FP-7 REDNEX Project and the Canada Research Chairs Program. The experimental work was funded by a consortium of DEFRA, BBSRC, the Milk Development Council, Purina Mills LLC, and NUTRECO Inc.

References

Berthiaume, R., Thivierge, M.C., Patton, R.A., Dubreuil, P., Stevenson, M., McBride, B.W., Lapierre, H., 2006. Effect of ruminally protected methionine on splanchnic metabolism of amino acids in lactating dairy cows. J. Dairy Sci. 89, 1621-1634.

Cantalapiedra-Hijar, G., Lemosquet, S., Rodriguez-Lopez, J.M., Messad, F., Ortigues-Marty, I., 2014. Diets rich in starch increase the posthepatic availability of amino acids in dairy cows fed diets at low and normal protein levels. J. Dairy Sci. 97, 5151-5166.

Connell, A., Calder, A.G., Anderson, S.E., Lobley, G.E., 1997. Hepatic protein synthesis in the sheep: effect of intake as monitored by use of stable-isotope-labelled glycine, leucine and phenylalanine. Br. J. Nutr. 77,255-271.

Crompton, L.A., France, J., Reynolds, C.K., Mills, J.A.N., Hanigan, M.D., Ellis, J.L., Bannink, A., Bequette, B.J., Dijkstra, J., 2014. An isotope dilution model for partitioning phenylalanine and tyrosine uptake by the mammary gland of lactating dairy cows. J. Theor. Biol. 359, 54-60.

Dijkstra, J., Oenema, O., Van Groenigen, J.W., Spek, J.W., van Vuuren, A.M., Bannink, A., 2013. Diet effects on urine composition of cattle and N_2O emissions. Animal 7 (suppl. 2), 292-302.

420 Doelman, J., Curtis, R.V., Carson, M., Kim, J.J.M., Metcalf, J.A., Cant, J.P., 2015. Essential
421 amino acid infusions stimulate mammary expression of eukaryotic initiation factor 2Bε but
422 milk protein yield is not increased during an imbalance. J. Dairy Sci. 98:4499-4508.
423 Doepel, L., Hewage, I.I., Lapierre, H., 2016. Milk protein yield and mammary metabolism
424 are affected by phenylalanine deficiency but not by threonine or tryptophan deficiency. J.
425 Dairy Sci. 99, 3144-3156.
426 France, J., Hanigan, M.D., Reynolds C.K., Dijkstra J., Crompton, L.A., Maas J.A., Bequette,
427 B.J., Metcalf J.A., Lobley, G.E., MacRae, J.C., Beever, D.E., 1998. An isotope dilution
428 model for partitioning leucine uptake by the bovine liver. J. Theor. Biol. 198, 121-133.
429 Harris, P.A., Skene, P.A., Buchan, V., Milne, E., Calder, A.G., Anderson, S.E., Connell, A,
430 Lobley, G.E., 1992. Effect of food intake on hind-limb and whole-body protein
431 metabolism in young growing sheep: chronic studies based on arterio-venous techniques.
432 Br. J. Nutr. 68, 389-407.
433 Hristov, A.N., Price, W.J., Shafii, B., 2004. A meta-analysis examining the relationship
434 among dietary factors, dry matter intake, and milk and milk protein yield in dairy cows. J.
435 Dairy Sci. 87, 2184-2196.
436 Katz, M.L., Bergman, E.N., 1969. Simultaneous measurements of hepatic and portal venous
437 blood flow in the sheep and dog. Am. J. Physiol. 216, 946-952.
438 Larsen, M., Galindo, C., Ouellet, D.R., Maxin, G., Kristensen, N.B., Lapierre, H., 2015.
439 Abomasal amino acid infusion in postpartum dairy cows: Effect on whole-body,
440 splanchnic, and mammary amino acid metabolism. J. Dairy Sci. 98, 7944-7961.
441 Matthews, D.E., 2007. An overview of phenylalanine and tyrosine kinetics in humans. J.
442 Nutr. 137, 1549S-1555S.
443 Rafii, M., McKenzie, J.M., Roberts, S.A., Steiner, G., Ball, R.O., Pencharz, P.B., 2008. *In*
444 *vivo* regulation of phenylalanine hydroxylation to tyrosine, studied using enrichment in

apoB-100 In vivo regulation of phenylalanine hydroxylation to tyrosine, studied using enrichment in apoB-100. Am J Physiol Endocrinol Metab, 294(2), E475-E479.

Raggio, G., Lobley, G.E., Berthiaume, R., Pellerin, D., Allard, G., Dubreuil, P., Lapierre, H., 2007. Effect of protein supply on hepatic synthesis of plasma and constitutive proteins in lactating dairy cows. J. Dairy Sci. 90, 352-359.

Reynolds, C.K., 2006. Splanchnic metabolism of amino acids in ruminants, in: Sejrsen, K., Hvelplund, T., Nielsen, M.O., (Eds), Ruminant Physiology: Digestion, metabolism and impact of nutrition on gene expression, immunology and stress. Wageningen Academic Press, Wageningen, the Netherlands, pp. 225-248.

Rulquin, H., Pisulewski, P., 2000. Effects of duodenal infusions of graded amounts of Phe on mammary uptake and metabolism in dairy cows. J. Dairy Sci. 83(Suppl. 1), 267-268.

Tagari, H., Webb Jr., K., Theurer, B., Huber, T., DeYoung, D., Cuneo, P., Santos, J.E.P., Simas, J., Sadik, M., Alio, A., Lozano, O., Delgado-Elorduy, A., Nussio, L., Nussio, C., Santos, F., 2004. Portal drained visceral flux, hepatic metabolism, and mammary uptake of free and peptide-bound amino acids and milk amino acid output in dairy cows fed diets containing corn grain steam flaked at 360 or steam rolled at 490 g/L. J. Dairy Sci. 87, 413-430.

Tagari, H., Webb Jr., K., Theurer, B., Huber, T., DeYoung, D., Cuneo, P., Santos, J.E.P., Simas, J., Sadik, M., Alio, A., Lozano, O., Delgado-Elorduy, A., Nussio, L., Bittar, C.M.M., Santos, F., 2008. Mammary uptake, portal-drained visceral flux, and hepatic metabolism of free and peptide-bound amino acids in cows fed steam-flaked or dry-rolled sorghum grain diets. J. Dairy Sci. 91, 679-697.

UniProt Consortium, 2017. UniProt: the universal protein knowledgebase. Nucleic Acids Res. 45, D158-D169.

Waterlow, J.C. 2006. Protein turnover. CAB International, Wallingford, UK.

Table 1. Principle symbols used for the kinetic model.

F_{ij}	Flow of PHE[a] or TYR[a] to pool i from j; F_{i0} denotes an external flow into pool i and F_{0j} denotes a flow from pool j out of the system	μmol/min
I_i	Effective rate of constant infusion of ^{13}C labelled PHE or TYR into primary pool i	μmol/min
Φ_i	Effective rate of constant infusion of ^{2}H labelled TYR into primary pool i	μmol/min
Q_i	Quantity of PHE[a] or TYR[a] in pool i	μmol
q_i	Quantity of ^{13}C labelled PHE or TYR in pool i	μmol
ϕ_i	Quantity of ^{2}H labelled TYR in pool i	μmol
e_i	Enrichment of ^{13}C PHE or TYR in pool i: ($= q_i/Q_i$)	atoms % excess/μmol
ε_i	Enrichment of ^{2}H TYR in pool i: ($=\phi_i/Q_i$)	atoms % excess/μmol
t	Time	min

[a]Total material (*i.e.* tracee + tracer).

475 **Table 2.** Experimental and other inputs.
476

Cow		323/14	341/29	6031/42	6132/43[a]
Dietary CP (g/kg)		175	128	128	175
Milk yield (kg/d)		25.8	24.1	24.2	25.3
Plateau	e_1	2.19	3.37	2.79	2.10
enrichment (APE)	e_2	3.58	5.51	4.31	3.32
	e_3[b]	0.15	0.18	0.18	0.32
	e_4[b]	0.28	0.30	0.30	0.43
	e_6[b]	1.07	1.65	1.29	1.00
	e_7[b]	0.08	0.09	0.09	0.13
	e_9	2.14	3.54	2.70	2.00
	e_X[b]	0.25	0.32	0.28	0.39
	ε_3	0.76	1.16	0.85	0.79
	ε_4	1.12	1.97	1.21	1.15
	ε_7[b]	0.34	0.59	0.36	0.35
	ε_X	0.73	1.23	0.83	0.74
Flow (μmol/min)	I_1	52.6	44.5	53.7	56.9
	I_2	24.2	36.6	16.5	9.55
	Φ_3	19.0	12.2	16.5	16.3
	Φ_4	8.49	10.4	4.99	2.72
	F_{05}	33.8	33.8	33.8	33.8
	$F_{07}^{(o)}$	211	146	351	525
	F_{08}	25.0	25.0	25.0	25.0
	F_{09}	2595	1777	1938	2473
	F_{0X}	2858	1399	2034	2012

477
478 [a]Essential amino acid infusion
479 [b]Initial value
480
481

Table 3. Phenylalanine and tyrosine uptake and partition by the liver for four lactating dairy cows obtained using the ten-pool model (symbols are defined in the text and Table 1).

Cow		323/14	341/29	6031/42	6132/43
Flow (μmol/min)	F_{10}	2403	1319	1921	2711
	F_{20}	676	665	382	288
	F_{30}	2486	1048	1951	2072
	F_{40}	756	530	414	237
	$\overline{F_{56}-F_{65}}$	33.8	33.8	33.8	33.8
	$\overline{F_{87}-F_{78}}$	25.0	25.0	25.0	25.0
	F_{X7}	547	308	215	300
	F_{X4}	534	412	287	187
	F_{X3}	1778	679	1532	1525
	F_{73}	708	369	419	547
	F_{74}	223	118	127	50
	$F_{07}^{(s)}$	2323	1225	1713	1476
	F_{76}	138	70	172	332
	F_{70}	2037	1147	1586	1397
	F_{91}	1597	967	1366	1935
	F_{92}	449	487	272	205
	F_{96}	548	323	300	333
	F_{61}	806	353	555	776
	F_{62}	227	178	110	82
	F_{06}	2455	1568	2071	2444
	F_{60}	2143	1465	1911	2284
Adjusted	e_3[a]	0.19	0.19	0.16	0.25
plateau	e_4[a]	0.32	0.38	0.35	0.54
enrichment (APE)	e_6[a]	0.81	1.09	0.79	0.61
	e_7[a]	0.10	0.11	0.11	0.16
	e_X[a]	0.20	0.23	0.18	0.26
	ε_7[a]	0.25	0.39	0.22	0.21

[a]Final value

Table 4. Average slope (%) for each of the flows calculated by the model obtained by perturbing each input in turn[a].

Flow	Unperturbed (μmol/min)[b]	Input perturbed[c]																		
		e_1	e_2	e_3	e_4	e_6	e_7	e_9	e_X	ε_3	ε_4	ε_7	ε_X	I_1	I_2	Φ_3	Φ_4	F_{05}	$F_{07}^{(o)}$	F_{08}	F_{09}	F_{0X}
F_{10}	2086													1.0								
F_{20}	547														1.0							
F_{30}	1862															1.0						
F_{40}	519																1.0					
$\overline{F_{56}-F_{65}}$	34																	1.0				
$\overline{F_{87}-F_{78}}$	25																			1.0		
F_{X7}	260			-7.6	-3.4		-0.64		9.2	16	3.8	0.62	-16									1.0
F_{X4}	309			-8.5	-3.8		-0.71		10	5.2	1.2	0.20	-5.2									1.0
F_{X3}	1522			3.0	1.4		0.25		-3.7	-3.8	-0.91	-0.15	3.8									1.0
F_{73}	341			-13	-6.1		-1.1		16	17	4.1	0.65	-17			5.5						-4.5
F_{74}	210			12	5.6		1.0		-15	-7.7	-1.8	-0.29	7.6				2.5					-1.5
$F_{07}^{(s)}$	1626							0.18		3.8	1.6	-1.2	-4.2			3.8	1.6		-0.18	-0.02		-4.2
F_{76}	136			-3.3	-1.9	-1.0	2.1		4.1	6.6	2.8	-2.1	-7.4			3.3	1.0					-3.3
F_{70}	1512			0.30	0.17	0.09	-0.19		-0.37	3.5	1.5	-1.1	-3.9			2.6	1.3					-2.9
F_{91}	1488	-1.0	-0.41			-0.08		1.5						0.33	-0.33						1.0	
F_{92}	391	-1.0	-0.41			-0.08		1.5						-0.68	0.67						1.0	
F_{96}	366	5.2	2.1			0.39		-7.5						-0.64	0.63						1.0	
F_{61}	598	2.5	1.0			0.19		-3.6						2.7	0.82						-2.5	
F_{62}	157	2.5	1.0			0.19		-3.6						1.7	1.8						-2.5	
F_{06}	2163	3.1	1.3	0.21	0.12	-1.1	-0.13	-3.3	-0.26	-0.42	-0.18	0.14	0.46	3.1	1.3	-0.21	-0.06	-0.02			-3.3	0.21
F_{60}	1944	3.4	1.4			-1.2		-3.6						2.3	1.2						-2.5	

[a] The slope for each flow is expressed relative to the value of the flow obtained when no perturbation is made. Only slopes which differ from zero are shown.
[b] Values calculated from the mean of inputs reported in Table 2.
[c] Model solved by perturbing each input in turn by 0%, ±10% and ±20%.

Figure 1. Scheme for the uptake and utilisation of PHE and TYR by the liver of lactating dairy cows: (a) total PHE and TYR, (b) [^{13}C] labelled PHE and TYR and (c) [^{2}H] labelled TYR. Nomenclature is defined in Table 1. Represented pools are numbered 1 to X and labelled in Figure 1a. The small circles in Figure 1a indicate flows out of the system which need to be measured experimentally.

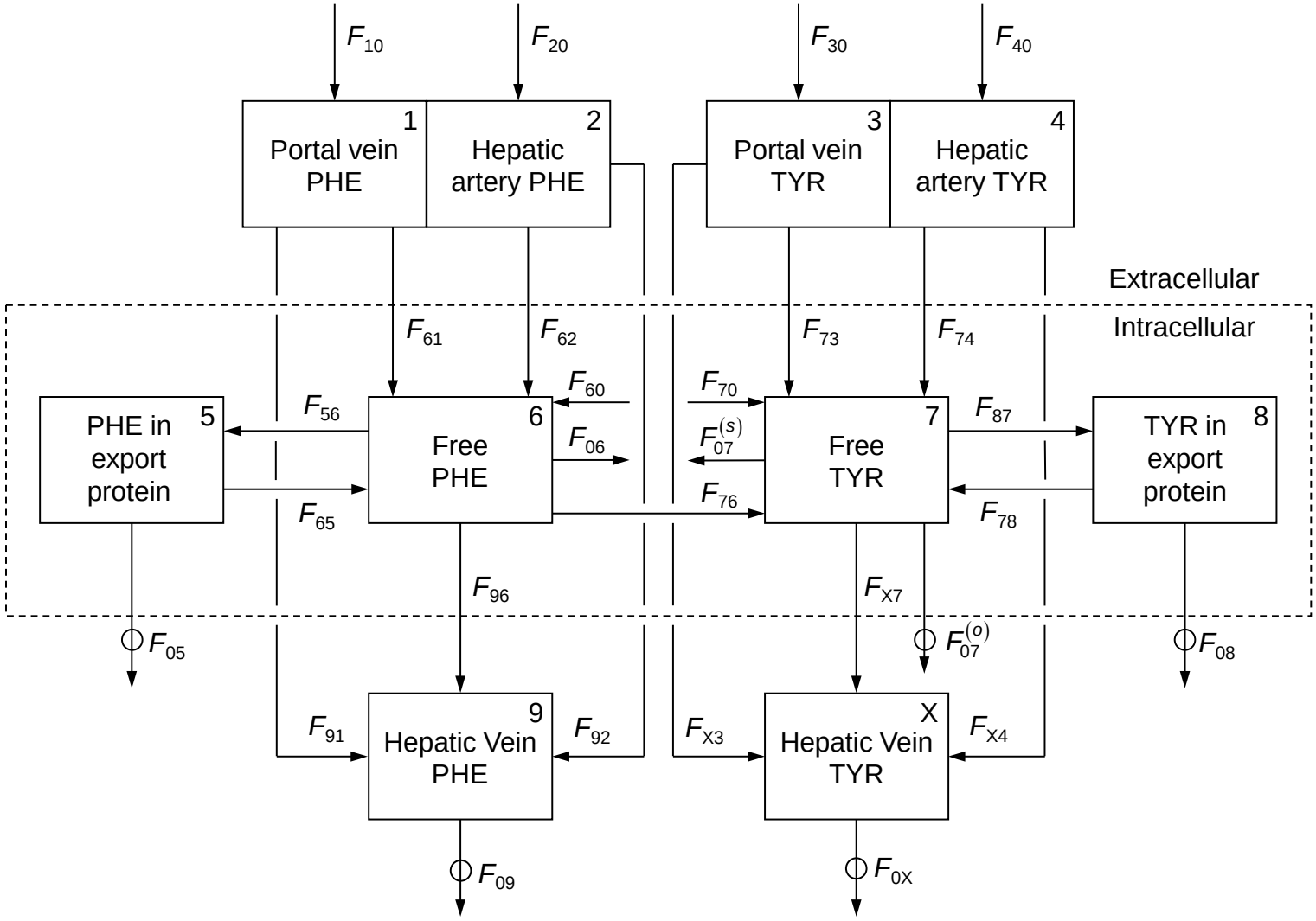

(a)

498

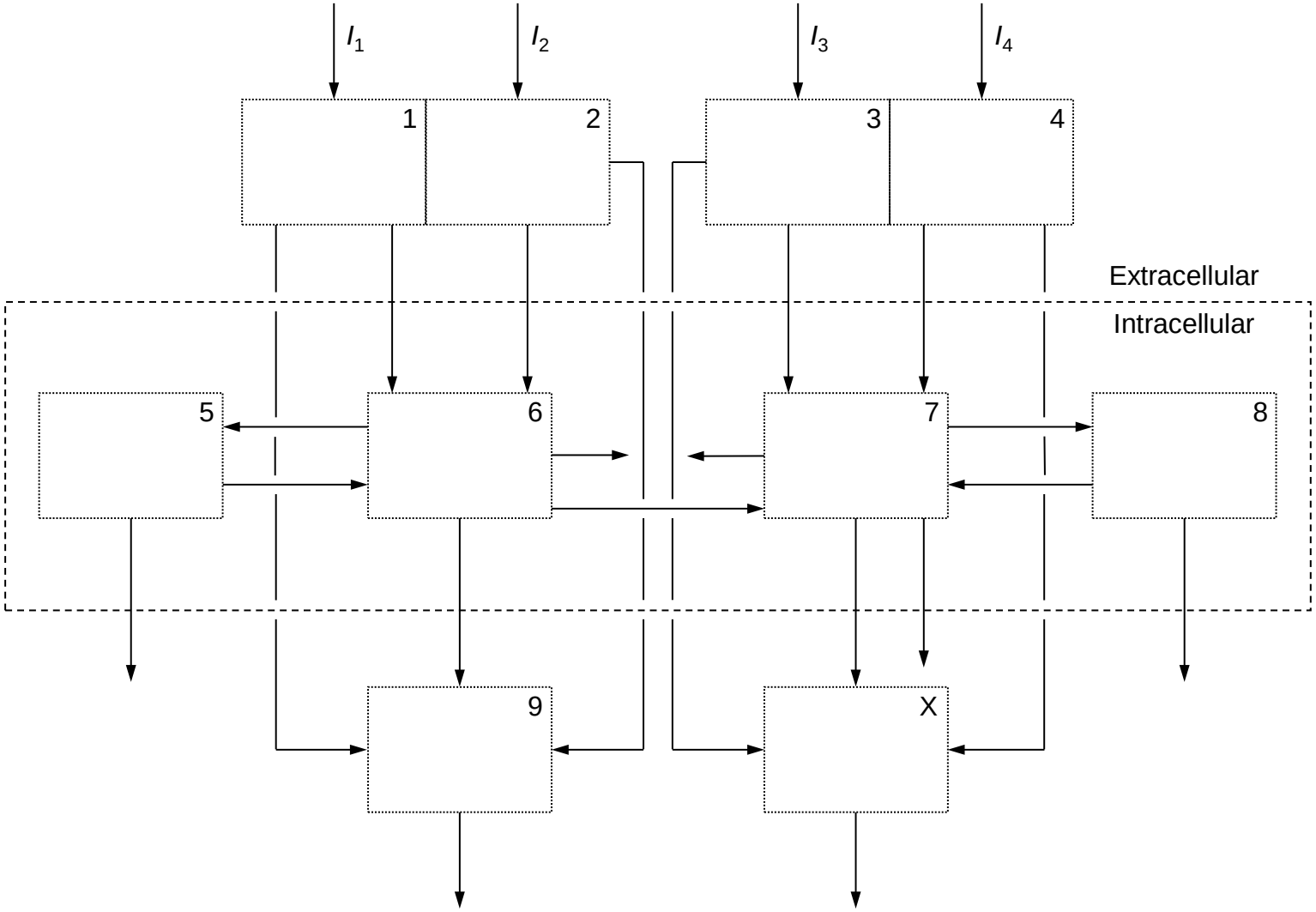

499 (b)

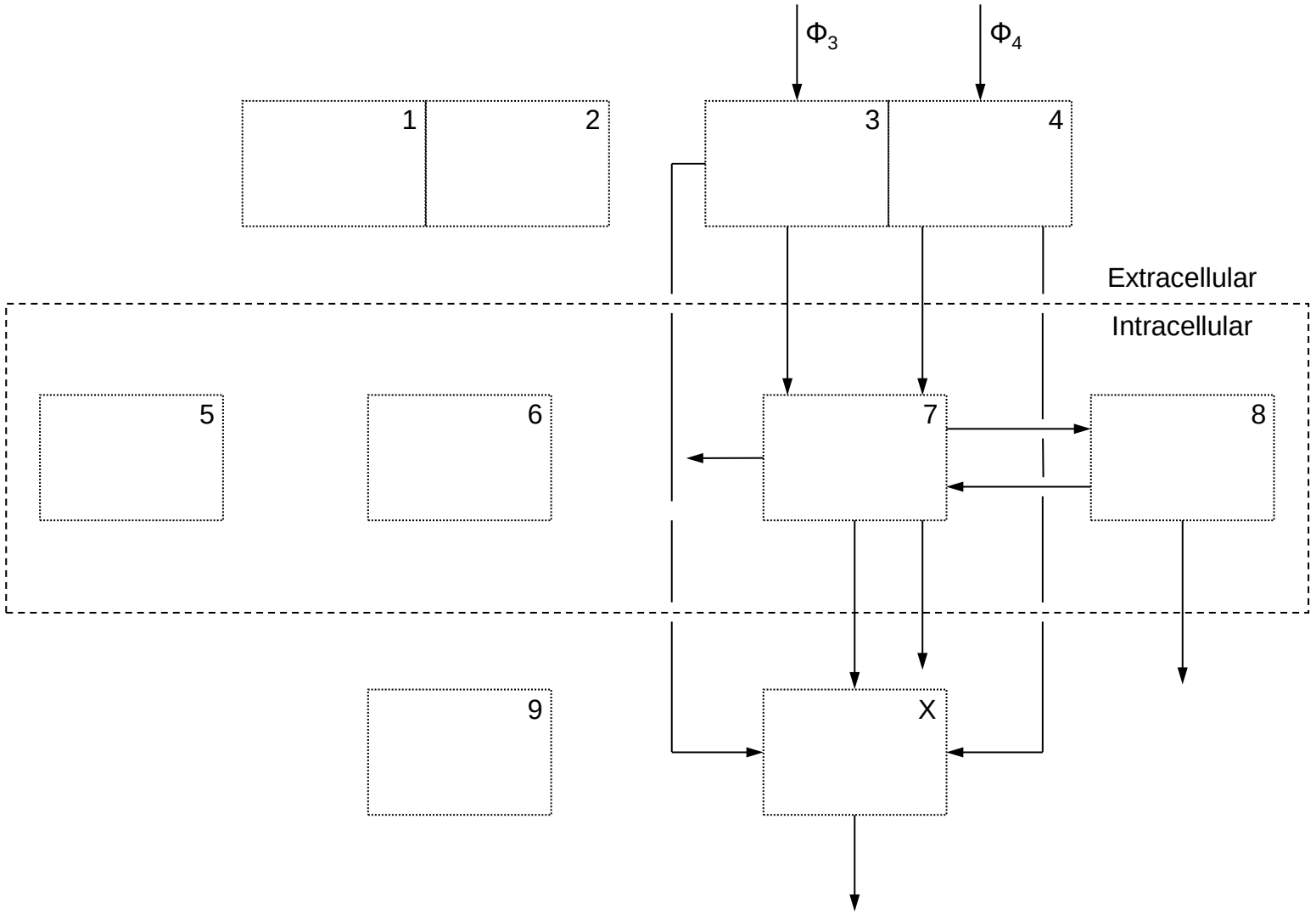

500 (c)